HIGH-DENSITY NEURAL MICROELECTRODE ARRAYS WITH COMPLEMENTARY WEDGE-SHAPED 3D ASSEMBLY INTERFACES FOR BRAIN ACTIVITY RECORDING

Liang Geng, Yujie Yang, Dongcheng Xie, Dongliang Chen, Lei Xu, and Feng Wu
University of Science and Technology of China, Hefei, CHINA

ABSTRACT

This paper introduces a high-density neural microelectrode array with a complementary wedge-shaped 3D assembly interface. The design incorporates five 2D neural probe chips, which are bonded to a flexible printed circuit (FPC) using an anisotropic conductive film (ACF) that features a complementary inverted trapezoidal interface. This approach results in a 3D neural microelectrode array consisting of 1280 microelectrodes, achieving both high-density integration and superior conduction efficiency in the 3D assembly. The two-dimensional neural probe chip integrates 256 microelectrodes within a 1.33 mm^2 area by making the microelectrodes protrude on the probe surface through a three-layer composite metal structure. The results from electrochemical impedance spectroscopy (EIS) reveal that the complementary wedge-shaped three-dimensional interface achieves exceptional uniformity and 100% conduction efficiency. Furthermore, after applying gold plating to modify the electrode surface, the AC impedance at 1K Hz decreases significantly from 1.58 MΩ to 206 KΩ.

KEYWORDS

MEMS, neural microelectrode arrays, 3D assembly, high-density.

INTRODUCTION

The brain, a complex network, has around 100 billion neurons, each with thousands of synapses, forming an intricate nervous system. While individual neurons can be complex information-processing units in their own right, it is their synaptic connectivity patterns that allow neurons to form specialized circuits for specific functions, making the brain a powerful computational device[1]. To reveal the functional mechanisms of the brain and decipher the neuronal loop mechanisms, the electrical activity of individual neurons needs to be observed and recorded simultaneously as much as possible[2, 3], and the dynamic processes of a large number of neurons at the millisecond scale during brain function[4], which requires technical means of observing the brain with millisecond temporal resolution and spatial resolution that can be recorded to individual neurons at the same time, and existing techniques for observing and recording brain activity signals techniques include functional magnetic resonance imaging, two-photon calcium imaging, voltage-sensitive imaging, and neuronal extracellular electrophysiology[5]. Currently, the only available techniques for directly detecting extracellular electrical signals from individual neurons with high spatial and temporal resolution are multichannel neurophysiological recording methods[6]. To capture the electrical signals issued by individual neurons on a large scale, the development of high-density neural microelectrodes is essential.

Microelectrodes are the gold standard technique for recording action potentials, and invasive microelectrodes have the spatiotemporal resolution to record action potential delivery from individual neurons[7]. Invasive microelectrodes are available as flexible electrodes and rigid electrodes. Flexible electrodes are microelectrodes with a biocompatible flexible polymer substrate material, which is suitable for long-term recording. However, the low Young's modulus of the substrate material results in poor localization accuracy during implantation. Rigid electrodes made from rigid metal or silicon-based semiconductor substrates can achieve higher density electrode integration with high surgical implantation accuracy[8]. Electrodes fabricated by CMOS or MEMS planar process technology are only distributed in one plane, and two-dimensional microelectrodes need to be encapsulated in three dimensions into neural microelectrode arrays before they have a three-dimensional spatial resolution. The neural electrodes and signal processing circuits monolithically integrated with the CMOS process to acquire over 900 channels are active electrodes that generate heat for a long time doing electrophysiological recordings[9]. Currently, neural microelectrodes processed with microelectromechanical systems (MEMS) technology are still an important experimental tool for the neuroscience community[10].

DESIGN AND FABRICATION

A good research experience in making 3D neural electrodes by the method of MEMS process has been reported in the past[11], and recent studies have been conducted to bond flexible cables with silicon-based 2D neural microelectrode probes by hot-pressing them through ACF(adhesive conductive film) before 3D stacking into neural microelectrode arrays. Optimization work on 3D packaging of 2D neural probes was reported [12, 13], where rows of grooves were etched around the bonding pads of 2D neural probes to assist in achieving planar bonding. The thermocompression bonding interface pads of these works are arranged in a matrix, and such a structure inevitably causes the metal interconnection lines of the 2D neural probe to overlap with the metal interconnection lines of the flexible cable when ACF thermocompression bonding is performed. This is due to the conductive metal particles of the ACF film having diameters in the micron scale, which are much larger than the thickness of the surface insulation layer of the neural probe. The metal interconnection lines of the flexible cable and the bonding pads are in the same plane. Since the conductive particles of the ACF film are uniformly distributed, there are also conductive particles between the overlapping interface of

the metal interconnection line of the neural probe chip and the metal interconnection line of the flexible cable. During the hot-pressure bonding process, the conductive particles at the overlapping interface will burst due to thermal pressure, leading to fatal short-circuit problems. Based on this, the matrix pad of the bonding interface of the neural microelectrode needs to be coated with a layer of metal bumps with a thickness of more than 100 microns to form a sufficient height gradient between the metal interconnection line of the 2D neural probe and the matrix pad of the bonding interface[11], thus avoiding the risk of short circuit caused by the bursting of the ACF conductive particles at the overlapping interface by thermal pressure, which is a complicated process with poor consistency and high experimental costs. Highly challenging to scale up to higher density neural electrodes.

Although the process of plating metal bumps on the bonding pads of low-density neural microelectrodes can be temporarily eliminated by etching deep grooves around the bonding pads of the probes to make the bonding pads relatively convex, this optimization scheme does not address the short-circuit risks that may be caused by the overlap of the metal interconnection lines of the 2D neural probes with the metal interconnection lines of the flexible cables in the matrix bonding interface pad structure, and the short-circuit risks that may be caused by the overlap of the metal interconnection lines of the flexible cables in the higher density neural probes. Furthermore, under the bonding pad interface of higher density neural electrodes, it is difficult to have enough space for etching deep trench isolation grooves around the bonding pad[12].

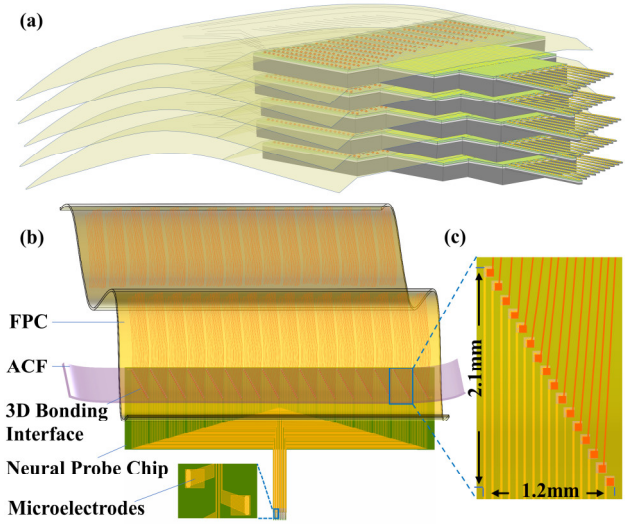

Figure 1: Schematic of 3D neural microelectrode arrays with the complementary wedge-shaped assembly interfaces.

In this work, we have optimized the bonding pad interface structure between the neural probe chip and the flexible cable, as shown in Figure 1(b), and we have developed a neural microelectrode chip with a complementary wedge-shaped 3D bonding interface. The pads of the three-dimensional complementary wedge-shaped interface of the neural probe chips are arranged in an oblique stepped pattern, and this structure makes the metal interconnection lines of the neural probes and the metal interconnection lines of the FPC in opposite directions. A detailed view of the complementary wedge interface can be seen in Figure 1(c). Due to the complementary structure, the whole bonding interface has no overlapping interfaces except for the overlapping pads that need to be bonded, which completely utilizes the bonding interface area and saves nearly 50% of the interface area. More importantly, since there is no overlapping interface, only the pads to be bonded can touch each other in the Z-axis direction during anisotropic conductive film (ACF) bonding, which makes it unnecessary to plate metal bumps or other post-treatment processes on the bonded pads.

Figure 1(a) is a schematic diagram of a high-density three-dimensional neural microelectrode array. The microelectrode array consists of five two-dimensional neural probe chips that have completed ACF hot-press bonding, stacked in parallel in the Z-axis direction, totaling 1280 microelectrodes. Each hot-press bonded neural probe chip has a thickness of no more than 700 microns. The shanks of the two-dimensional neural probe chips are 5.0 to 5.3 mm long, and the microelectrode covers a depth of 0.8 to 1.3 mm.

There are two design structures: one with four shanks and another with eight shanks. The four-shank structure is a tetrode with a lateral width of 0.98 mm, while the eight-shank structure is a polytrode with a lateral width of 1.0-1.1 mm. Each two-dimensional neural probe has 256 microelectrodes, and the three-dimensional microelectrode arrays enable high-density electrophysiological recordings across multiple brain regions simultaneously.

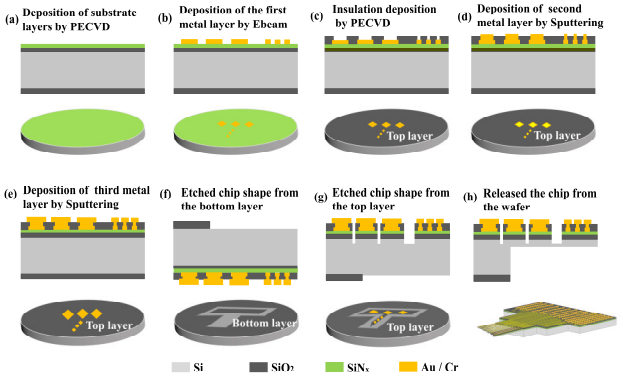

Figure 2: The key MEMS fabrication process.

The fabrication steps of the proposed neural probe chips using typical MEMS process are shown in figure 2.

a. The front side deposits silicon oxide and silicon nitride as substrate layers on a silicon wafer (100) by PECVD. Backside deposits silicon oxide as a mask layer.
b. Deposition of the first metal layer on the front side by e-beam.
c. Deposition of insulating layer by PECVD and etching of microelectrodes and bonding pads by RIE (reactive ion etching) .
d. Deposition of a second interconnect metal layer by sputtering.
e. Deposition of a third contact metal layer by sputtering.
f. Etching the back side silicon oxide mask layer by RIE and releasing the outline of the neural probe chip.

g. Etching the front substrate layer by RIE and ICP (inductively coupled plasma) to release the neural probe outline.
h. Etching the silicon on the backside by ICP, releasing the neural probe chip.

RESULTS AND DISCUSSION

Figure 3 displays the completed fabricated neural probe chip. The two-dimensional neural probe chip employs a three-layer metal structure. When the number of microelectrode channels increases to high-density electrodes, over 60% of the probe's lateral width is occupied by metal interconnection lines. As the number of electrode channels grows, the proportion of the lateral width occupied by microelectrodes decreases, with most of it being taken up by metal interconnection lines. Too large a lateral distance when implanting the electrode in a biological brain necessitates the design of as many microelectrodes as possible within the limited lateral width. Layering metal interconnects and microelectrodes can save some lateral width. The first metal layer is utilized for metal interconnection wire fabrication and microelectrode positioning, and the microelectrode positioning point can be the same size as the metal interconnection wire. While the second metal layer is responsible for filling the small windowed holes in the insulating layer, connecting the first metal layer and the third contact metal layer. As depicted in Figure 3(f), the third metal layer serves as the contact metal layer on the electrode chip surface, enabling the microelectrode area to be expanded appropriately. This layered design of the metal layer allows microelectrodes to protrude from the probe surface and not to be on the same plane with the metal interconnection line. This increases the number of nerve electrodes per unit area while also augmenting the surface area of the electrodes and reducing the distance between the electrodes and the nerve cells. Such a configuration is beneficial for decreasing the AC impedance and enhancing the charge storage capacity of the microelectrodes.

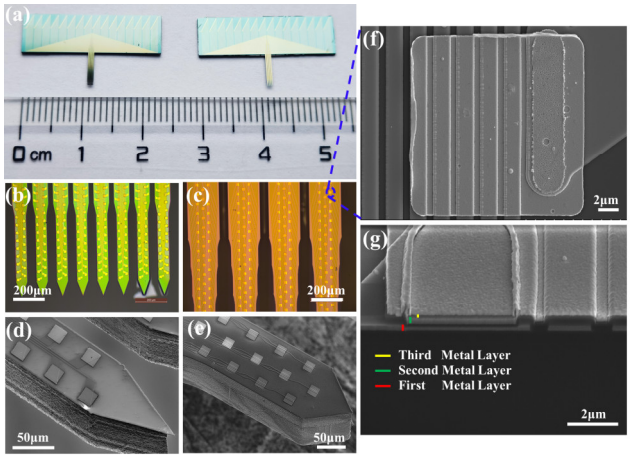

Figure 3: (a) 2D neural probe chip. (b) Polytrode type of microelectrodes with 8 shanks. (c) Tetrode type of microelectrodes with 4 shanks. (d) SEM of the Polytrode type microelectrodes. (e) SEM of the Tetrode type microelectrodes. (f) SEM of the single microelectrodes. (g) SEM image of Cross-sectional view of a single microelectrode through FIB.

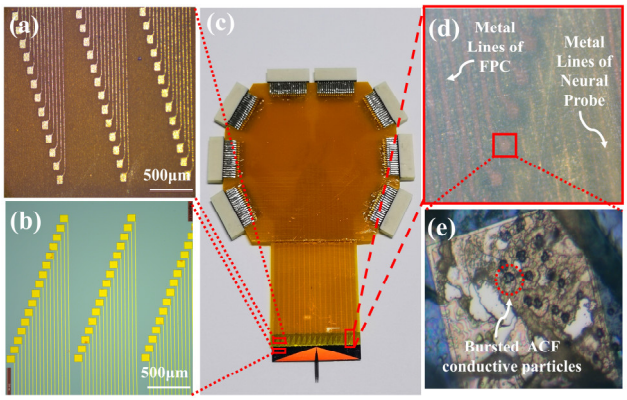

Figure 4: (a) Wedge-shaped bonding interface for FPC. (b) Wedge-shaped bonding interface for neural probe chip. (c) Complete ACF bonding of neural probe chip. (d) View of complete ACF bonded wedge-shaped interface. (e) Bursted ACF conductive particles.

Figure 4(c) presents the 256-channel neural probe chip that has completed ACF thermocompression bonding. The complementary wedge-shaped bonding interface between the probe chip and the flexible cable is displayed in Figures 4(a) and 4(b), which is designed to save bonding area and eliminate the risk of short circuits. Figure 4(e) depicts a microscopic image of the conductive particles of the ACF adhesive film, which have successfully undergone thermocompression bursting. A gap of approximately 45 degrees can be observed in the conductive particles, generally considered an indication of successful thermocompression bursting and good electrical conductivity.

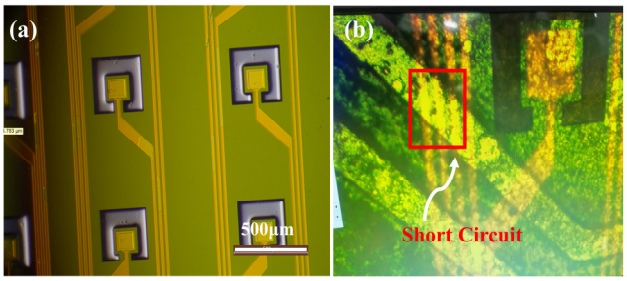

Figure 5: (a) Matrix Interface. (b) Matrix interface short-circuited during ACF bonding

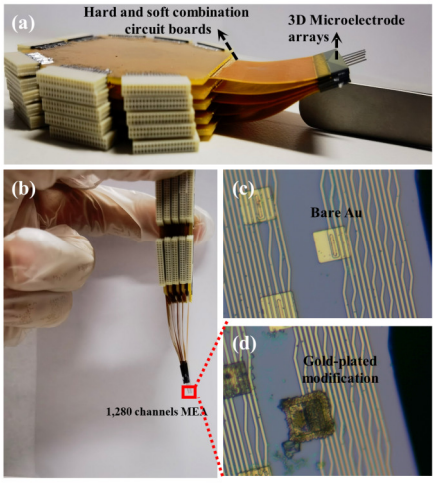

Figure 6: (a) 3D neural microelectrode arrays with 1,280 channels. (b) Handheld effect. (c) Microelectrode with bare Au. (d) Microelectrode with gold-plated modification.

Figure 5(a) depicts a matrix-type interface, whereas Figure 5(b) illustrates the ACF conductive particles pressing through the insulating layer, resulting in the short-circuit of the chip and FPC. The 1280-channel high-density neural microelectrode arrays were successfully assembled in three dimensions, as shown in Figure 6(a)(b). To enhance the recording performance of the microelectrodes, surface modification was conducted by electroplating gold onto their surface. The electrochemical impedance spectra were characterized before and after the surface modification, as displayed in Figure 7. Figure 7(c) presents the cyclic voltammetry measurements (25 mV/s, -1 volt to 1 volt) of Bare Au and Gold-plated after surface modification, indicating that Gold-plated has a greater charge storage capacity than Bare Au. Moreover, the AC impedance at 1 KHz is reduced from 1.5 MΩ to 200 KΩ, as demonstrated in Figure 7(a).

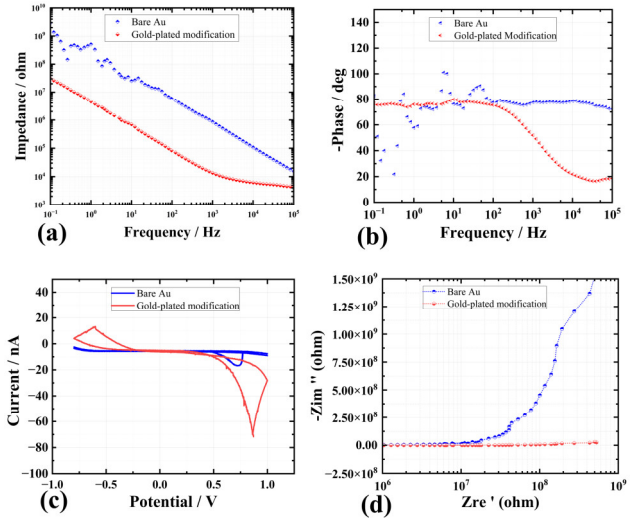

Figure 7: The electrochemical characterization of microelectrode with bare Au and gold-plated modification: (a) EIS diagrams. (b) Frequency and negative phase relationship. (c) CV diagrams. (d) Nyquist plot.

CONCLUSION

In this paper, we present a neural microelectrode array that features a complementary wedge-shaped 3D assembly bonding interface with 1280 microelectrodes. This result enables simultaneous large-scale recording of electrical activity in various brain regions. The proposed bonding interface has nearly 100% bonding conduction efficiency without the risk of short circuits and does not require any special process modification for the electrodes. In addition, this interface supports the expansion of higher density neural microelectrodes.

ACKNOWLEDGEMENTS

This work was supported by the National Key Research and Development Program of China (No. 2018YFE0194500), the National Natural Science Foundation of China (No. 31827803) and the Fundamental Research Funds for the Central Universities. We are also thankful for the fabrication platform supported by the USTC Center for Micro and Nanoscale Research and Fabrication.

REFERENCES

[1] L. Luo, "Architectures of neuronal circuits," *Science,* vol. 373, no. 6559, p. eabg7285, Sep 3 2021.

[2] A. P. Alivisatos, "The Brain Activity Map Project and the Challenge of Functional Connectomics," *Neuron,* vol. 74, no. 6, pp. 970-974, Jun 21 2012.

[3] G. Buzsaki, "Neural Syntax: Cell Assemblies, Synapsembles, and Readers," *Neuron,* vol. 68, no. 3, pp. 362-385, Nov 4 2010.

[4] J. Z. Young, "Foundations of the Neuron Doctrine - Shepherd,Gm," *Nature,* vol. 356, no. 6370, pp. 624-625, Apr 16 1992.

[5] A. Grinvald and R. Hildesheim, "VSDI: A new era in functional imaging of cortical dynamics," *Nat Rev Neurosci,* vol. 5, no. 11, pp. 874-885, Nov 2004.

[6] F. P. Battaglia and M. J. Schnitzer, "Editorial overview: Large-scale recording technology: Scaling up neuroscience," *Curr Opin Neurobiol,* vol. 32, pp. Iv-Vi, Jun 2015.

[7] G. S. Hong and C. M. Lieber, "Novel electrode technologies for neural recordings (vol 20, pg 330, 2019)," *Nat Rev Neurosci,* vol. 20, no. 6, pp. 376-376, Jun 2019.

[8] E. Musk and Neuralink, "An Integrated Brain-Machine Interface Platform With Thousands of Channels," *J Med Internet Res,* vol. 21, no. 10, p. e16194, Oct 31 2019.

[9] J. J. Jun *et al.*, "Fully integrated silicon probes for high-density recording of neural activity," *Nature,* vol. 551, no. 7679, pp. 232-+, Nov 9 2017.

[10] J. P. Seymour, F. Wu , "State-of-the-art MEMS and microsystem tools for brain research," *Microsyst Nanoeng,* vol. 3, Jan 2 2017.

[11] G. Rios, E. V. Lubenov, D. Chi, M. L. Roukes, "Nanofabricated Neural Probes for Dense 3-D Recordings of Brain Activity," *Nano Lett,* vol. 16, no. 11, pp. 6857-6862, Nov 2016.

[12] L. C. Wang, Z. J. Guo, B. W. Ji, Y. Xi, B. Yang, and J. Q. Liu, "A High-Density Drivable Microelectrodes Array for Multi-Brain Recording," *Int Sol St Sen Act M (*Transducers 2021*),* pp. 679-682, 2021.

[13] M. H. Wang *et al.*, "A novel assembly method for 3-dimensional microelectrode array with micro-drive," *Sensor Actuat B-Chem,* vol. 264, pp. 100-109, Jul 1 2018.

CONTACT

*Lei Xu, Email: okxulei@ustc.edu.cn.